Journal of Magnetism and Magnetic Materials 414 (2016) 82–89

Contents lists available at ScienceDirect

Journal of Magnetism and Magnetic Materials

journal homepage: www.elsevier.com/locate/jmmm

Ferromagnetism and strong magnetic anisotropy of the $PbMnBO_4$ orthoborate single crystals

A. Pankrats [a,b], K. Sablina [a], M. Eremin [c], A. Balaev [a], M. Kolkov [a,b,*], V. Tugarinov [a], A. Bovina [a]

[a] Kirensky Institute of Physics, Russian Academy of Sciences, Siberian Branch, Krasnoyarsk 660036, Russia
[b] Siberian Federal University, Krasnoyarsk 660041, Russia
[c] Institute of Physics, Kazan Federal University, Kazan 420008, Russia

ARTICLE INFO

Article history:
Received 18 September 2015
Received in revised form
1 April 2016
Accepted 16 April 2016
Available online 19 April 2016

Keywords:
Strong ferromagnetic anisotropy
Ferromagnetic resonance
Exchange interactions

ABSTRACT

The $PbMnBO_4$ orthoborate single crystals were first grown and their magnetic properties and ferromagnetic resonance were studied. It was found that the ferromagnetic state below the Curie temperature $T_C=31$ K is characterized by the strong magnetic anisotropy. The significant effective anisotropy fields of $PbMnBO_4$ determine the energy gap in the FMR spectrum, which is extraordinary large for ferromagnets (112 GHz at $T=4.2$ K). It was shown that the static Jahn–Teller effect characteristic of the Mn^{3+} ion leads to both the ferromagnetic ordering and the strong magnetic anisotropy in the crystal. In the strong external magnetic field the induced ferromagnetic ordering is retained in the crystal above the Curie temperature up to the temperatures multiply higher than T_C. A weak anomaly of the dielectric permittivity was observed in $PbMnBO_4$ at the Curie temperature at which the long-range ferromagnetic order is established.

1. Introduction

The search for new materials and study of their physical properties is one of the priorities of modern solid state physics. It is aimed at finding advanced materials for engineering applications and providing experimental data for studying new physical effects that arise at the intersection of magnetic, electrical, elastic, and other properties.

The $PbMnBO_4$ crystal belongs to a relatively new family of $PbMBO_4$ orthoborates whose structure for M=Ga, Al was first studied in [1]. Afterwards, the authors of this study investigated the magnetic properties of the isostructural series of polycrystalline samples with M=Fe, Cr, and Mn and established antiferromagnetic properties of the compositions with Fe^{3+} and Cr^{3+} ions and ferromagnetic properties of the composition with Mn^{3+} ions [2]. The strong dependence of the type of magnetic order on the kind of magnetic ion M stimulated us to investigate in detail the magnetic properties of these compounds. Note that the ferromagnetic order is extremely rarely met in oxide dielectrics and $PbMnBO_4$ is the only ferromagnet in this family.

Another stimulus for these investigations was a stereochemical feature of the Pb^{2+} ion. The electronic structure of this ion is characterized by the unusual electron density distribution caused by outer $6s^2$ electrons, which are not involved in the formation of a chemical bond and create isolated (lone) pairs [3]. These pairs strongly affect the ionic coordination and can lead to the occurrence of ferroelectric, nonlinear optical, and other interesting properties of the investigated crystals. Many compounds containing the stereochemical Pb^{2+} and Bi^{3+} ions with lone pairs, including $PbVO_3$ [4], $BiMnO_3$ [5], $BiFeO_3$ [6], and $Pb_3Mn_7O_{15}$ [7], exhibit the multiferroic properties.

Investigations of single-crystal samples yield more information on characteristics of materials, e.g., on their magnetic anisotropy. As a rule, it is convenient to study the physical properties of new compounds on their single crystals, since the latter have high quality. High-purity single crystals can be obtained when their chemical composition includes potential solvents, such as PbO, B_2O_3 and Bi_2O_3 oxides or their combinations. Using spontaneous crystallization by a flux technique, we synthesized $PbFeBO_4$ single crystals and established that their magnetic behavior [8] strongly differs from that of polycrystalline samples [2]. We showed that the features of magnetic behavior of polycrystalline samples are caused by the contribution of a concomitant *hematite* phase.

In addition, we investigated the dielectric properties of $PbFeBO_4$ [8] and found anomalies for both polycrystalline and single-crystal samples at the temperature of short- and long-range antiferromagnetic ordering, which indicates the correlation

* Corresponding author at: Kirensky Institute of Physics, Russian Academy of Sciences, Siberian Branch, Krasnoyarsk 660036, Russia.
E-mail addresses: pank@iph.krasn.ru (A. Pankrats), maxim_91@mail.ru (M. Kolkov).

http://dx.doi.org/10.1016/j.jmmm.2016.04.042
0304-8853/

between the magnetic and electrical subsystems in the crystals.

In this work, $PbMnBO_4$ single crystals were grown using spontaneous crystallization by a flux technique. Study of their magnetic and resonance properties revealed the strong magnetic anisotropy induced by the Jahn–Teller effect (JTE) associated with the Mn^{3+} cation. In addition, this effect explains the ferromagnetic order in the crystal. Preliminary investigations of the dielectric properties of $PbMnBO_4$ single crystals showed a weak permittivity anomaly at the Curie temperature at which the long-range ferromagnetic order is established.

2. Experimental

$PbMnBO_4$ single crystals were grown using spontaneous crystallization by a flux technique from high-quality Mn_2O_3, PbO, and B_2O_3 components taken in the stoichiometric ratio. The eutectic composition in the PbO–B_2O_3 system (93.7 wt% PbO and 6.3 wt% B_2O_3) with the melting point T_m=460 °C [9] was used as a solvent. The thoroughly mixed composition was placed into a platinum crucible and heated to 1000 °C. After exposure at this temperature for 2 h, the crucible was cooled to 500 °C at a rate of 3 °C/h. Then, the synthesized crystals were mechanically withdrawn from the crucible. They had a plate shape and a size of up to 4 × 2.5 × 0.5 mm^3. The crystals with a size of no more than 1 mm were transparent and red colored.

Studies on a Bruker D8 ADVANCE X-ray diffractometer and a Bruker SMART APEX II single crystal X-ray diffractometer confirmed the orthorhombic structure (sp. gr. *Pnma*) of the crystal and allowed us to determine orientations of the sample crystals axes. The obtained lattice constants a=6.70 Å, b=5.94 Å, and c=8.64 Å are consistent with the data reported in [2]. The crystal structure is similar to that of other orthoborates [2] and consists of chains of edge-sharing MnO_6 octahedra extended along the ***b*** axis. The MnO_6 octahedra in $PbMnBO_4$ are more distorted than in the orthoborates with M=Fe, Cr, Ga, and Al due to the JTE associated with the $3d^4$ Mn^{3+} cation. The chains are bridged by BO_3 orthoborate groups forming a three-dimensional $MnBO_4^{2-}$ framework. The Pb^{2+} cations occupy asymmetric 4-fold coordination sites typical of stereoactive pairs with s-orbitals and fill the empty [010] tunnels in the structure.

It was established that the plate crystal plane can be oriented parallel to either (011) or (101) crystallographic plane; the longer plate side coincides with the ***a*** or ***b*** orthorhombic axis. Figs. 1a and 1b show XRD spectra for the (011) and (101) planes, respectively. The indexed peaks correspond to reflections from the respective crystal planes. The rest peaks belong to the cell where the sample is placed. Fig. 1c shows the X-ray spectrum of the cell, which forms a background in Figs. 1a and b. The data obtained showed no twinning and confirmed high crystal quality of the samples. The magnetic properties of the crystals of both types were found to be similar.

The magnetic measurements were performed on an original vibrating sample magnetometer in the temperature range from 4.2 to 300 K and magnetic fields of up to 70 kOe. Ferromagnetic resonance (FMR) study of the $PbMnBO_4$ single crystals was carried out on an original magnetic resonance spectrometer with the broad frequency band (25–140 GHz) and pulsed magnetic fields of up to 90 kOe [10].

The dielectric properties of the samples were investigated on an Agilent E4980A LCR meter in the frequency range from 10 kHz to 2 MHz. The investigated sample was a polycrystalline pill 5 mm in diameter sintered from grinded single crystals. Electrodes were formed from a silver paste deposited onto the pill faces.

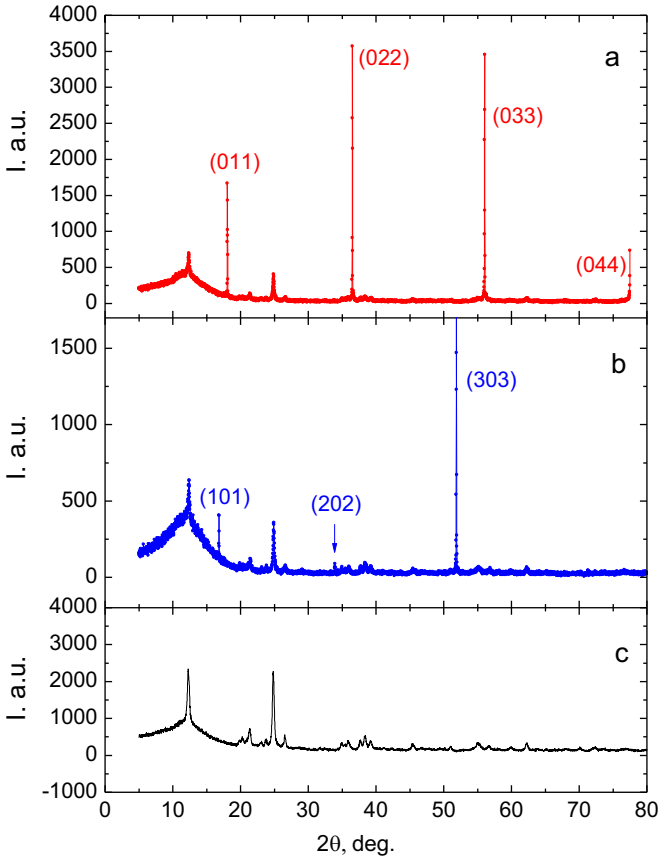

Fig. 1. (a, b) XRD spectra for two planes of the $PbMnBO_4$ single crystals and (c) XRD spectrum for the cell.

3. Results and discussion

3.1. Magnetic properties

Temperature dependences of magnetic susceptibility for the $PbMnBO_4$ single crystal measured along all the orthorhombic crystal axes in a magnetic field of 1 kOe are presented in Fig. 2. The Curie temperature T_c=31 K determined from the sharp susceptibility drop at H||a (dashed line in the Fig. 2) is consistent with the data for the polycrystalline sample [2]. Note that the susceptibility along the ***a*** axis below T_c is noticeably higher that along the other

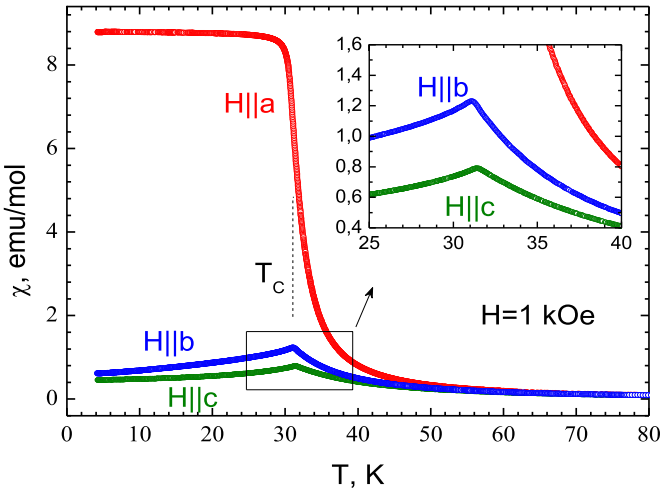

Fig. 2. Temperature dependences of the magnetic susceptibilities measured along the orthorhombic axes, H=1 kOe.

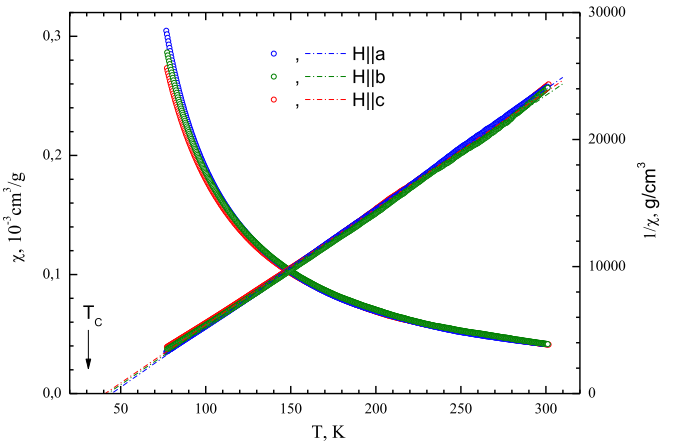

Fig. 3. Temperature dependences of magnetic susceptibility along the orthorhombic axes. $H=1$ kOe.

two directions, where establishment of the magnetic order is accompanied by the pronounced sharp peak of the susceptibility. Fig. 3 shows temperature dependences of magnetic susceptibility along all the orthorhombic axes in the paramagnetic temperature range and a magnetic field of 1 kOe. At $T>150$ K, all the dependences are well described by the Curie-Weiss law, in contrast to the data from [2] where the magnetic susceptibility contains a significant temperature-independent contribution and the temperature dependence of $1/\chi$ is nonlinear. The calculated dependences for inverse magnetic susceptibility $1/\chi$ are shown in the Fig. 3 by dashed lines. The effective magnetic moments $\mu_a=5.3\mu_B$, $\mu_b=5.4\mu_B$, and $\mu_c=5.4\mu_B$ are slightly higher than the theoretically predicted value $4.9\mu_B$ for the Mn^{3+} ion. The paramagnetic Curie temperatures $\theta_a=42$ K, $\theta_b=45$ K, and $\theta_c=41$ K are positive and slightly higher than T_C. In the paramagnetic state, a weak anisotropy of magnetic susceptibility is observed only below 140 K.

It follows from the data in Fig. 2 that the magnetic anisotropy is much stronger in the ordered state.

To study the anisotropic properties of the $PbMnBO_4$ crystal, we measured field dependences of magnetization in the three orthorhombic directions at different temperatures (Fig. 4). According to these dependences, the easy magnetization direction coincides with the orthorhombic ***a*** axis in consistence with the neutron data [2]. The saturation magnetization 3.92 μ_B at $T=4.2$ K agrees well with the theoretical value 4.0 μ_B for the ferromagnetically ordered Mn^{3+} ions. Along the orthorhombic ***b*** axis, the magnetization saturates in a magnetic field of 20.6 kOe at $T=4.2$ K. The orthorhombic ***c*** axis is the hardest: the saturation magnetization field in this direction is 47.0 kOe at $T=4.2$ K. Temperature dependences of anisotropy fields H_{Ab} and H_{Ac} determined as saturation fields in the corresponding directions are shown in Fig. 5. The anisotropy fields decrease upon approaching Curie temperature T_C in the both hard directions. The strong anisotropy fields and their strong temperature dependences near T_C are responsible for susceptibility peaks that arise at the magnetic phase transition for the *b* or *c* directions. Upon cooling the crystal, the magnetization measured along one of the hard axes increases at approaching Curie temperature T_C, until the anisotropy field becomes much weaker than the measuring field. With a further decrease in temperature and an increase in the anisotropy field above the external magnetic field, the magnetic moments deviate toward the easy direction and reduce the magnetization measured along the hard direction. For the same reasons, the maximum value of the magnetization peak measured in the hardest ***c*** direction is smaller than that along the ***b*** axis.

In addition, it should be noted that the field dependences of magnetization remain weakly nonlinear even well above the Curie

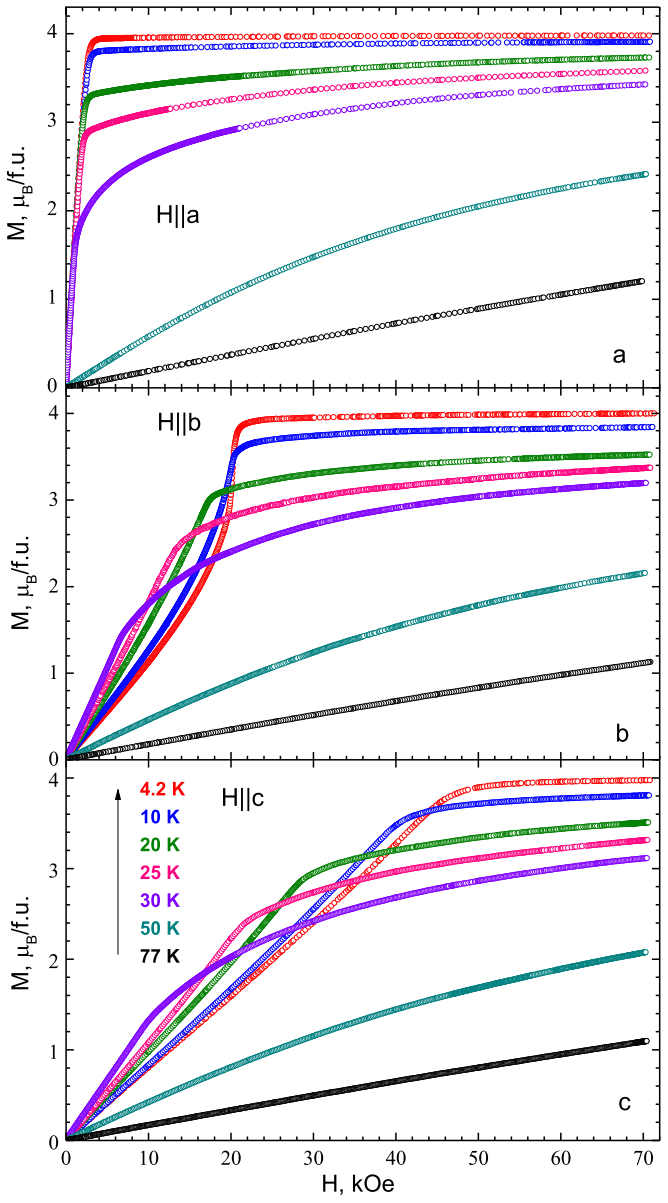

Fig. 4. Magnetic field dependences of the magnetizations measured along orthorhombic axes at various temperatures.

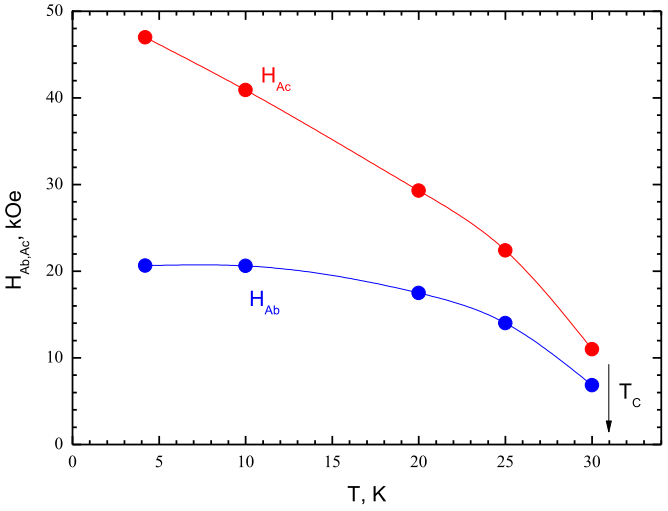

Fig. 5. Temperature dependences of magnetic anisotropy fields for the ***b*** and ***c*** axes.

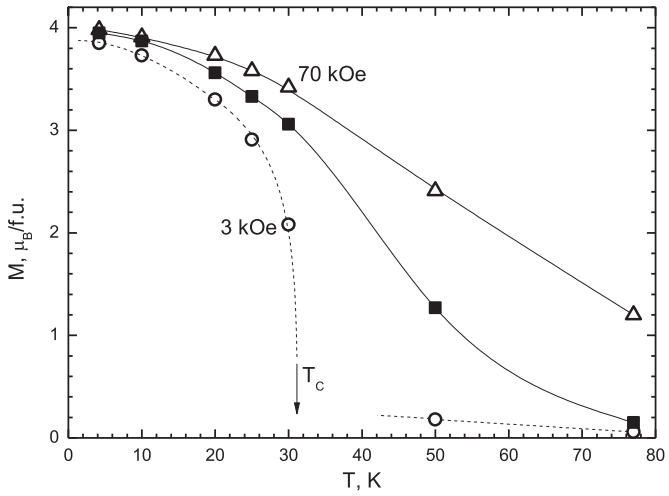

Fig. 6. Temperature dependences of magnetization along the ***a*** axis in magnetic fields of 3 (open circles) and 70 kOe (open triangles) and of saturation magnetization (closed squares).

temperature up to the maximum measuring temperature (77 K). The induced ferromagnetic ordering is apparently conserved in the crystal above the Curie temperature due to the strong external magnetic field.

The measuring field strongly affects temperature dependences of magnetization. Fig. 6 shows temperature dependences of magnetization measured in the easy direction in fields of 3 (circles) and 70 kOe (triangles). Closed squares show the temperature dependence of saturation magnetization in the easy direction obtained from the linear strong-field portions of the magnetization curves in Fig. 4a by approximation to the field $H=0$. The resulting curves are strongly different. The temperature dependence measured in a field of 3 kOe is typical of ferromagnets; the sharp magnetization drop is observed upon approaching the Curie temperature. With an increase in the measuring field, the magnetic phase transition becomes increasingly spread; the magnetic field-induced magnetization takes large values at temperatures far above than T_C.

The magnetic hysteresis loop was measured along the easy direction of the single-crystal sample (Fig. 7a) and in the disc-shaped polycrystalline sample sintered from ground $PbMnBO_4$ single crystals (Fig. 7b). When the single crystal is magnetized along the orthorhombic ***a*** axis, we can see a narrow hysteresis loop caused only by the domain wall motion. The low coercive field ($H_c=50$ Oe at $T=4.2$ K) is indicative of a small number of domain wall pinning centers due to the high quality of the synthesized single crystals. In the polycrystalline sample prepared by grinding of the same single crystals, the coercive field increases to 1.5 kOe due to the random orientation of grains in the polycrystal and the significant number of pinning centers arising at the grain boundaries. Note also that the magnetization curve for the polycrystalline sample has some features observed in magnetic fields corresponding to the anisotropy fields for the ***b*** and ***c*** axes. These features are shown by arrows in Fig. 7.

3.2. Ferromagnetic resonance

Ferromagnetic resonance study of the $PbMnBO_4$ single crystals was carried out using a magnetic resonance spectrometer at frequencies of 30–120 GHz in pulsed magnetic fields. The measurements were performed on single-crystal plates; the sample plane was parallel to both the (101) and (011) crystallographic planes; the FMR parameters for these two samples were the same.

Fig. 8 shows frequency-field FMR dependences measured at $T=4.2$ K along all the orthorhombic axes. It can be seen that the oscillation branches are softened in the fields of magnetization saturation in the hard directions, ***b*** and ***c***. The experimental data were approximated by the theoretical frequency-field dependences calculated for an orthorhombic ferromagnet in [11].

The frequency-field dependence is quasi-linear when magnetic field H is directed along the easy magnetization axis:

$$\nu = \gamma\sqrt{(H + H_{Ab})(H + H_{Ac})}, \tag{1}$$

where H_{Ab} and H_{Ac} are the anisotropy field in the ***b*** and ***c*** directions, respectively, and γ is the gyromagnetic ratio. For the magnetic field applied along one of the hard axes, e.g., ***b,*** we have

$$H < H_{Ab}, \quad \nu = \gamma\sqrt{H_{Ab}H_{Ac} - \frac{H^2 H_{Ac}}{H_{Ab}}}, \tag{2a}$$

$$H > H_{Ab}, \quad \nu = \gamma\sqrt{H + (H_{Ac} - H_{Ab})}\cdot\sqrt{H - H_{Ab}}. \tag{2b}$$

Similar dependences are obtained for the other hard axis at the replacement $H_{Ab} \leftrightarrow H_{Ac}$. The frequency-field dependences calculated for all the three orientations are shown by solid lines. The experimental data at $T=4.2$ K are described well using the parameters $\gamma=3.4$ MHz/Oe, $H_{Ab}=22.6$ kOe, and $H_{Ac}=47.5$ kOe. The obtained anisotropy fields are similar to the saturation fields obtained from the field dependences of magnetization for

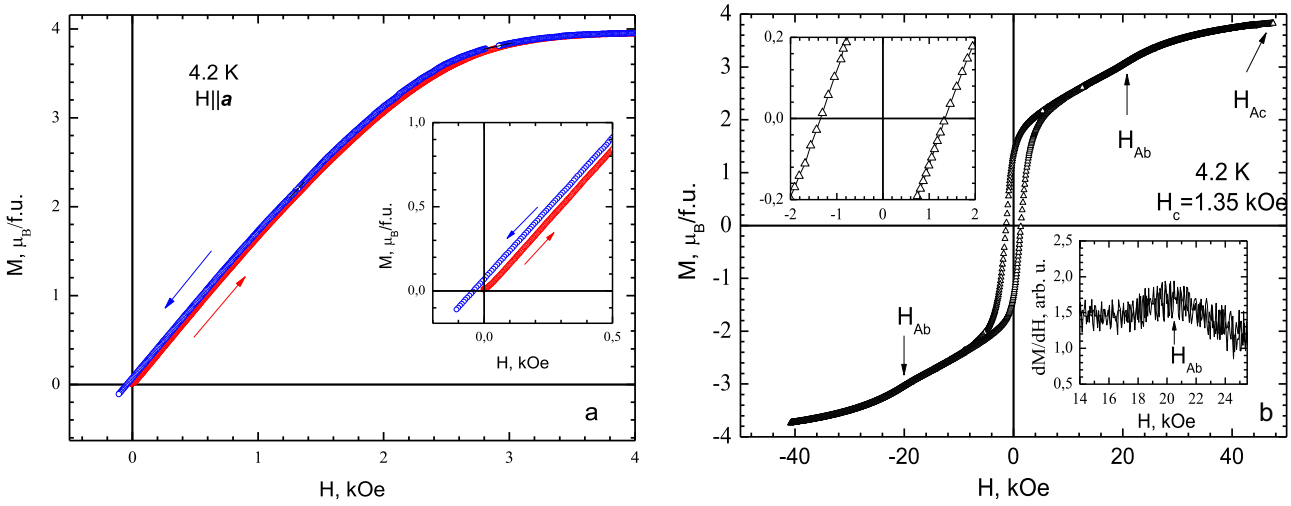

Fig. 7. Magnetic hysteresis measured at $T=4.2$ K (a) along the ***a*** axis of the single crystal and (b) in the polycrystalline sample.

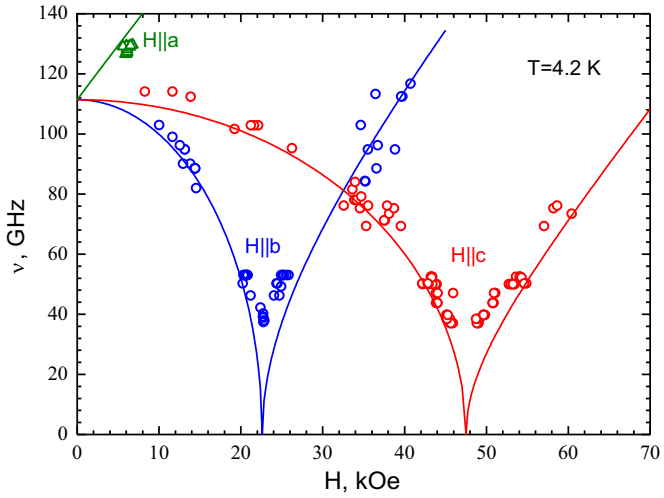

Fig. 8. Frequency-field dependences of FMR in $PbFeBO_4$ at $T=4.2$ K.

the corresponding magnetic field orientations. A minor discrepancy between the experimental and calculated dependences is caused by the sample orientation error.

Note that the resonance spectra are characterized by the same energy gap $\nu_c = \gamma\sqrt{H_{Ab}H_{Ac}} = 112$ GHz in all the three magnetic field orientations. Such a large value is atypical of a ferromagnet and originates from the strong magnetic anisotropy of $PbMnBO_4$.

Figs. 9a and b show temperature dependences of resonance field for the magnetic field directed along one of the hard axes and easy axis, respectively. At the orientation H||b (Fig. 9a), the resonance spectrum consists of two absorption lines (inset to Fig. 9a) with different temperature and frequency-field dependences. As the temperature is increased, the anisotropy field and, correspondingly, the energy gap of the spectrum decrease; therefore, taking into account the frequency-field dependence of the low-field line (see Fig. 8 and Eq. (2a)), its resonance field sharply decreases at a certain temperature. This line disappears when the gap becomes smaller than the measuring frequency, i.e., at $\nu_c < \nu = 49.11$ GHz. At the same time, the resonance field of the high-field line defined by Eq. (2b) monotonically decreases with increasing temperature. In contrast to ordinary ferromagnets, whose resonance field reaches a plateau defined by the expression $\nu = \gamma H$ near the Curie temperature, the resonance field of the $PbMnBO_4$ crystal continues decreasing well above the magnetic ordering temperature.

The temperature dependence of resonance field for the easy direction H||a is presented in Fig. 9b. In this case, the measuring frequency is lower than the initial spectrum splitting ν_c at $T=4.2$ K; therefore, the FMR absorption at this crystal orientation appears above the liquid helium temperature. With a further increase in temperature and a decrease in the energy gap, the resonance field monotonically grows. As in the previous case, the resonance field variation continues well above T_c. This temperature dependence of the resonance field is consistent with the established nonlinearity of the field dependences of magnetization observed above T_c and can also be explained by conservation of the induced ferromagnetic ordering above the Curie temperature in an external magnetic field. In the both figures, the dotted line shows the resonance field levels corresponding to the value $\gamma=2.8$ MHz/Oe. The comparison shows this level is attained at $T \approx 50$ K in magnetic fields of 17–20 kOe (Fig. 9a) and only near 80 K in fields above 30 kOe (Fig. 9b). Probably, the stronger the applied magnetic field, the wider the temperature range of conservation of the field-induced magnetically ordered state.

Fig. 10 shows the temperature dependence of energy gap ν_c in the spectrum calculated from the temperature dependence of the resonance field at H||a. As expected, the gap is nonzero above T_C and tends to zero at approaching a temperature of about 80 K.

Strictly speaking, the phase transition from the paramagnetic to ferromagnetic state occurs only at $H=0$, since in an applied magnetic field the induced magnetization is conserved above the Curie temperature; therefore, these two states have the same symmetries. In an applied magnetic field, the transition is spread not only in ferromagnets [12], but also in canted antiferromagnets [13], which also have a spontaneous magnetic moment. However, the field-induced ferromagnetic state is usually conserved above T_C by a few Kelvin degrees. In contrast to this case, the induced ferromagnetic order is conserved in $PbMnBO_4$ up to the temperatures multiply higher than T_C.

3.3. Dielectric properties

The dielectric properties of the $PbMnBO_4$ crystal were studied only on a polycrystalline pill, since it is impossible to perform dielectric measurements on an individual single crystal of such a small size. The measurements were performed in the frequency

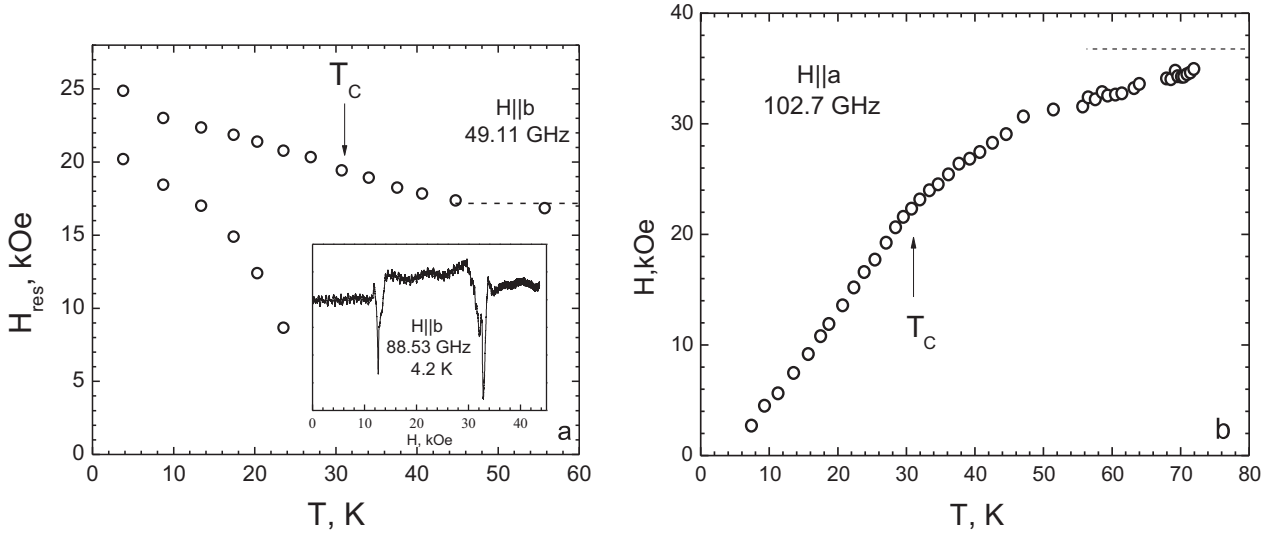

Fig. 9. Temperature dependences of resonance field measured for (a) H||b, $\nu=49.11$ GHz and (b) H||a and $\nu=102.8$ GHz. Inset: resonance spectrum for H||b and $\nu=88.53$ GHz at $T=4.2$ K.

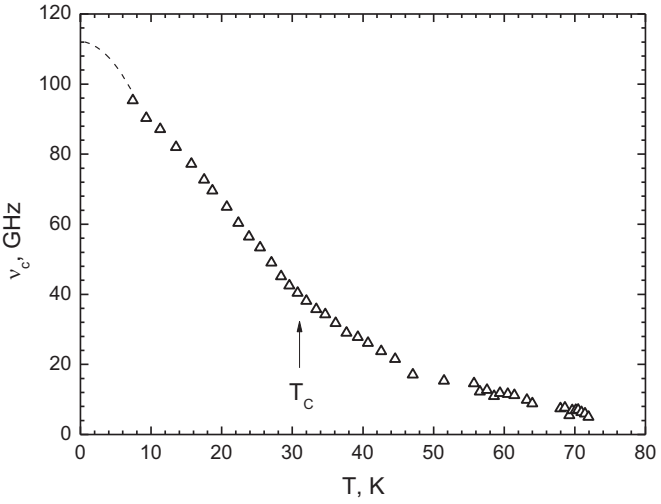

Fig. 10. Temperature dependency of the energy gap calculated from experimental data of Fig. 9b.

range from 1 kHz to 2 MHz at temperatures 4.2–100 K.

We expected the more pronounced magnetoelectric effect in ferromagnetic $PbMnBO_4$ than in antiferromagnetic $PbFeBO_4$, where we observed rather bright anomalies of the dielectric properties, including dielectric loss, at the magnetic phase transition. Unfortunately, the preliminary study of the dielectric properties of $PbMnBO_4$ did not meet these expectations. No noticeable anomalies of the dielectric loss were detected. The only weak anomaly of a capacitance determined from the real part of permittivity ε' was found near T_C. A fragment of one of the dependences measured at 200 kHz is shown in Fig. 11. The anomaly is observed in the form of a clear kink near T_C and is independent of an external magnetic field of 10 kOe applied parallel to the ac electric field.

Possibly, the anomalies of the dielectric properties would be more pronounced for a single crystal at proper magnetic and electric field orientations.

4. Discussion: the origin of ferromagnetism and strong magnetic anisotropy

The magnetic order in the $PbMnBO_4$ crystal is determined by two types of the exchange interactions. The exchange coupling between neighboring paramagnetic ions in a chain is indirect and acts through an $O3^{2-}$ ion. Fig. 12 shows fragments of the crystal structure. It can be seen that the indirect exchange interactions can couple adjacent chains through BO_3 and PbO_4 groups. To establish the ferromagnetic order in the crystal, both the intra- and interchain interactions should be ferromagnetic. It is very difficult to analyze the interchain exchange interaction via lead and boron ions. The exchange interactions in $PbMBO_4$ (M=Cr, Mn, Fe) were investigated in [14] using *ab-initio* calculations in the framework of the density functional theory (DFT). The calculations showed that the intrachain exchange interaction dominates in the $PbMBO_4$ crystals. Unfortunately, the DFT calculations do not explain why the ferromagnetic order exists only in the crystal with M=Mn. In our opinion, this is due to different degrees of distortions of the octahedra surrounding these ions. Structural studies of the crystals in this family showed [2] that the octahedra around Fe^{3+} and Cr^{3+} ions are slightly distorted, probably due to the effect of the stereoactive Pb^{2+} ion. At the same time, the oxygen octahedra surrounding the ion Mn^{3+} are distorted much stronger. The distances between M^{3+} ions and O^{2-} ions occupying three nonequivalent positions in the octahedron and the angles of M–O–M bonds through O3 and O1 ions are given in Table 1.

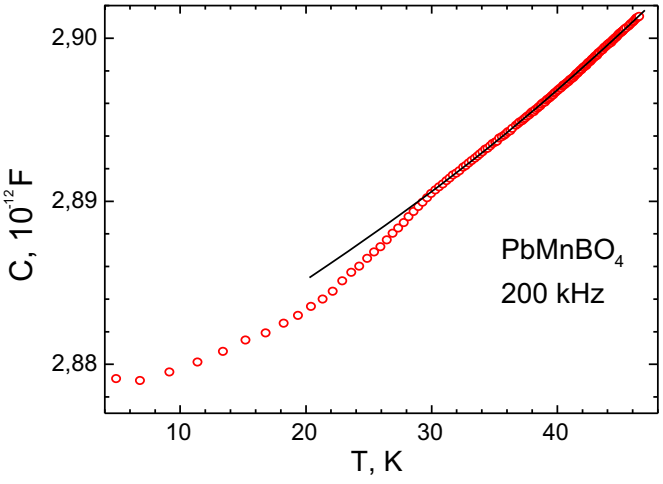

Fig. 11. Temperature dependence of capacitance of the $PbMnBO_4$ polycrystalline disk at 200 kHz.

It can be seen that at M=Mn, the oxygen octahedron is significantly extended in the O3 ion direction and the Mn–O1 bond, vice versa, is shorter than the oxygen environment of Fe^{3+} and Cr^{3+} ions. The angles of M–O–M bonds through these two oxygen ions also noticeably change.

Such a distortion is typical of the static JTE in the Mn^{3+} state [15]. The ground electronic configuration of a manganese ion in a strong crystal field is $Mn^{3+}(t_{2g}^3 e_g^1)$. Since the MnO_6 octahedron fragments are strongly distorted, we may conclude that e_g electrons occupy the $|3z^2 - r^2\rangle$ states. Here, we assume that the local z axis is directed along the Mn-O3 bond (bold line in Fig. 12). The most effective channel of superexchange between Mn ions via a bridging O3 ion can be easily explained. Indeed, the $|3z^2 - r^2\rangle_1$ state of a Mn1 ion (upper chain in Fig. 2) overlaps with the $|2p_z\rangle_1$ oxygen state of a O3 ion, whereas the $|3z^2 - r^2\rangle_2$ state of a Mn2 ion overlaps with the $|2p_z\rangle_2$ oxygen state of the same bridging O3 ion. Since the $|2p_z\rangle_1$ and $|2p_z\rangle_2$ oxygen states are nearly orthogonal, this superexchange channel, according to the Goodenough–Kanamori–Anderson rule [16–18], must be ferromagnetic.

Now, let us discuss the origin of the strong magnetic anisotropy. The main contribution is made by the crystal field, which results from the distorted octahedral coordination around Mn^{3+} ions. Indeed, the spin-spin and spin-orbit interactions (in the second-order perturbation theory) in the Jahn-Teller distorted MnO_6 fragment can be described using the effective Hamiltonian [15]

$$H_{\text{eff}} = D_{zz}S_z^2 + D_{xx}S_x^2 + D_{yy}S_y^2. \quad (3)$$

Here, the z axis is also directed along the Mn–O3 bond. The D_{zz} value for the $3d^4$ state is expected to be about $-2\ \text{cm}^{-1}$ [19]. Since this value is negative [15], the easy magnetization axis should coincide with the z axis. The preferred direction of Mn^{3+} spins in a Jahn–Teller distorted MnO_6 octahedron was discussed also by Whangbo et al. in [20].

The local z axes of neighboring Mn1 and Mn2 ions in a chain form an angle of 83.4°. Owing to both the ferromagnetic intrachain interaction and mutual rotation of the local z axes of octahedron fragments in each chain, the ***b*** components of the easy magnetization direction cancel out. Thus, the addition of components D_{zz} yields the resulting easy magnetization direction for each chain (dashed lines in Figs. 12a and b). It can be seen in Fig. 12b that the

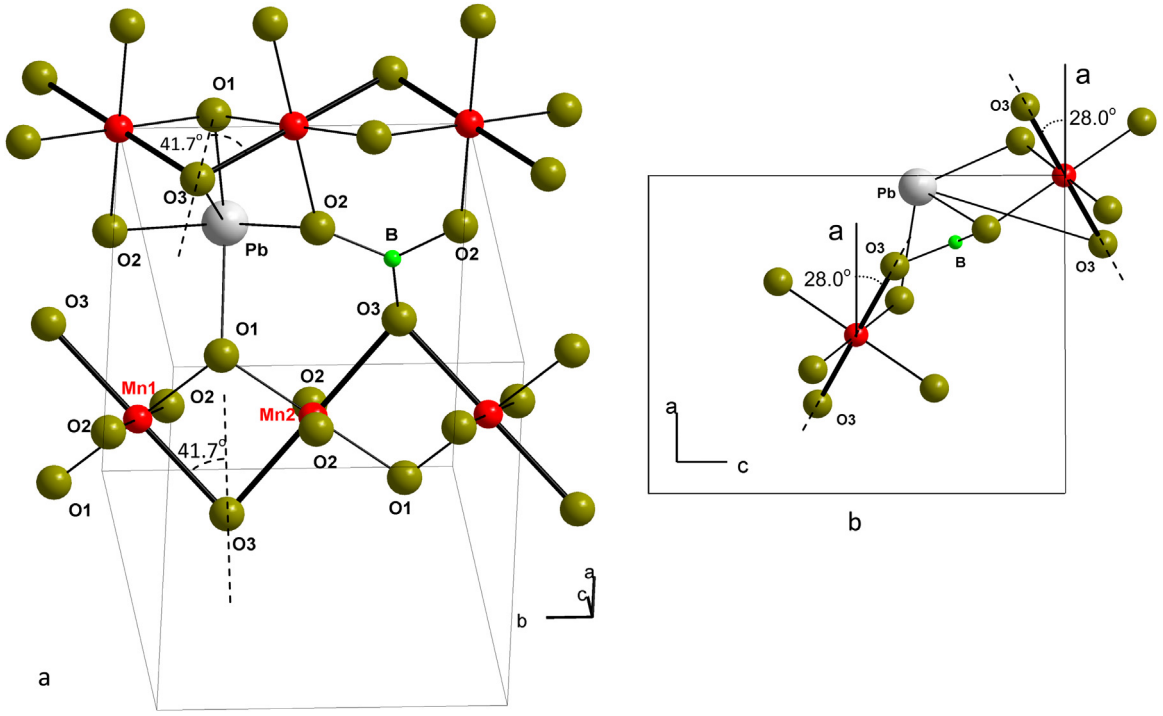

Fig. 12. a – fragment of the crystal structure of $PbMnBO_4$, b – view of two adjacent chains in ***ac***-plane.

Table 1
Bond distances and angles in $PbMBO_4$ [2].

Distances and angles	$PbFeBO_4$	$PbCrBO_4$	$PbMnBO_4$
M–O1, Å	1.923(3)	1.941(6)	1.885(3)
M–O2, Å	2.035(4)	1.989(6)	1.990(3)
M–O3, Å	2.095(4)	2.031(6)	2.225(4)
M–O1–M, deg.	101.2(2)	99.8(3)	104.0(2)
M–O3–M, deg.	90.2(2)	94.0(3)	83.8(2)

easy axes of neighboring chains are symmetrically rotated in the ***ac*** plane by an angle of 28.0° relative to the orthorhombic ***a*** axis. The interchain ordering is also ferromagnetic [14], which leads to the cancelling out of ***c*** components of the easy axes of neighboring chains. Eventually, the resulting easy magnetization direction of the entire crystal coincides with the orthorhombic ***a*** axis what is in accordance with the experimental data. The direction of the intermediate anisotropy axis is most likely determined by the positive contribution of the exchange link $|xy\rangle_1$-O3-$|3z^2 - r^2\rangle_2$ to D_{yy} and, probably, by the contribution of the dipole-dipole interaction.

5. Conclusions

The $PbMnBO_4$ orthoborate single crystals were first grown and their magnetic properties and ferromagnetic resonance were studied. It was found that the ferromagnetic state below the Curie temperature $T_C = 31$ K is characterized by the strong magnetic anisotropy. The easy magnetization axis coincides with the orthorhombic ***a*** axis, while the orthorhombic ***b*** and ***c*** axes are hard. The ***c*** axis is the hardest; the corresponding effective magnetic anisotropy field attains 47 kOe at $T = 4.2$ K.

The significant effective anisotropy fields of $PbMnBO_4$ determine the energy gap in the FMR spectrum, which is extraordinary large for ferromagnets (112 GHz at $T = 4.2$ K).

The magnetic and resonance studies showed that in an external magnetic field the induced ferromagnetic ordering is retained in the crystal above the Curie temperature up to the temperatures multiply higher than T_C.

It was found that the anomalies of dielectric properties observed in $PbMnBO_4$ at the established ferromagnetic order are much weaker than in the isostructural $PbFeBO_4$ antiferromagnet.

It was shown that the static Jahn-Teller effect characteristic of the Mn^{3+} ion leads to the ferromagnetic ordering in the $PbMnBO_4$ crystal. The same effect apparently causes the strong magnetic anisotropy in the crystal.

Acknowledgments

We acknowledge the assistance of A. Dubrovsky in magnetic measurements.

This work was supported by the Russian Foundation for Basic Research, Projects nos. 13-02-00897 and 16-02-00563. MVE thanks for support the Russian Government Program of Competitive Growth of the Kazan Federal University, decision no. 930_p, May 22, 2015.

References

[1] H. Park, J. Barbier, Acta Crystallogr. E57 (2001) 82.
[2] H. Park, R. Lam, J.E. Greedan, J. Barbier, J. Chem. Mater. 15 (2003) 1703.
[3] P.B. Moore, P.K. Sen Gupta, Y. Le Page, Am. Mineral. 74 (1989) 1186.
[4] R. Shpanchenko, V. Chernaya, A. Tsirlin, P. Chizhov, D. Sklovsky, E. Antipov, E. Khlybov, V. Pomjakushin, A. Balagurov, J. Medvedeva, E. Kaul, C. Geibel, Chem. Mater. 16 (2004) 3267.
[5] T. Atou, H. Chiba, K. Oboyama, Y. Yamaguchi, Y. Syono, Solid State Chem. 145 (1999) 639.
[6] G.A. Smolenskii, J.E. Chupis, Sov. Phys. Uspekhi 25 (1982) 475.
[7] N. Volkov, E. Eremin, K. Sablina, N. Sapronova, J. Phys.: Condens. Matter 22 (2010) 375901.
[8] A. Pankrats, K. Sablina, D. Velikanov, A. Vorotynov, O. Bayukov, A. Eremin, M. Molokeev, S. Popkov, A. Krasikov, J. Magn. Magn. Mater. 353 (2014) 23.
[9] N.A. Toropov, V.P. Barzakovskii, V.V. Lapin, N.N. Kurtseva, State Diagrams of Silicate Systems, Nauka, Moscow-Leningrad, 1965, Reference book.
[10] V.I. Tugarinov, I. Ya Makievskii, A.I. Pankrats, Instrum. Exp. Tech. 47 (2004) 472.

[11] A.I. Pankrats, V.I. Tugarinov, K.A. Sablina, J. Magn. Magn. Mater. 279 (2004) 231.
[12] D.O. Smith, Phys. Rev. 102 (1956) 959.
[13] A.S. Borovik-Romanov, V.I. Ozhogin, JETP 39 (1960) 27.
[14] H.J. Koo, M.H. Whangboo, Sol. St. Commun. 149 (2009) 602.
[15] A. Abragam, B. Bleany, Electron Paramagnetic Resonance of Transition Ions, Clarenaon Press, Oxford, 1970.
[16] J.B. Goodenough, J. Phys. Chem. Solids 6 (1958) 287.
[17] J. Kanamori, J. Phys. Chem. Solids 10 (1959) 87.
[18] P.W. Anderson, Phys. Rev. 115 (1959) 2.
[19] K. Ono, S. Koide, H. Sekiyama, H. Abe, Phys. Rev. 96 (1954) 38.
[20] M.H. Whangbo, E.E. Gordon, H. Xiang, H.J. Koo, C. Lee, Acc. Chem. Res.. 48 (2015) 3080.